JOURNAL OF MATERIALS SCIENCE **36** (2001) 4845–4849

EBSP study of reaction zone in SiC/Al metal matrix composite prepared by laser melt injection

V. OCELÍK, J. A. VREELING, J. TH. M. DE HOSSON*
Department of Applied Physics, Materials Science Centre and Netherlands Institute for Metals Research, University of Groningen, Nijenborgh 4, 9747 AG Groningen, The Netherlands
E-mail: hossonj@phys.rug.nl

The reaction zone in SiC/Al metal matrix composite layer prepared by Laser Melt Injection process is studied by Electron Back-Scatter Diffraction. Special attention is dedicated to the sample preparation process and also to the automatic indexing procedure when patterns of back-scattered electrons are evaluated during the surface scanning by electron beam. The orientation relationship between ceramic particles and phase formed in the reaction zone was observed by both transmission electron microscopy and by EBSD.

1. Introduction

The injection of carbide particles into a melt pool, which is created in the top of a metal substrate by a high power laser [1, 2], may form Metal Matrix-ceramic Composite (MMC) layers on metal surfaces. The main goal of this Laser Melt Injection (LMI) process is to improve the mechanical and chemical properties of metal surfaces like Al, Ti and steels. Surface layers prepared by the LMI process exhibit strong bonding and no large discontinuity of properties at the layer/substrate interface.

The overall properties of the MMC layer depend on the specific properties and amount of injected carbide powder, on the microstructure of the laser beam re-melted substrates and on the presence and properties of new phases formed by chemical reactions between matrix and particles. These phases are mainly present at the particle/matrix interface in a so-called reaction zone. It was reported [3–5] before that the failure starts in this zone during mechanical or chemical testing of SiC/Al and SiC/Ti-alloy MMC layers.

The aim of this work was to study the orientation relationships between the SiC particle, the Al matrix and the Al_4C_3 plates [6] by Electron Back-Scattering Diffraction (EBSD) [7]. In particular we report on the sample preparation for EBSD, which is not straightforward.

2. Experimental

The LMI process was used to prepare single tracks of SiC/Al MMC using a 2 kW Rofin Sinar Nd : YAG laser. The mean particle size was 80 μm and the purity of Al was 99.6 wt %. A more detailed description of the laser injection process, particular the process parameters as well as a detailed description of the formed microstructure can be found elsewhere [2, 6].

Standard mechanical grinding (SiC papers up to 1200) and polishing (from 6 to 1 μm diamond and SiO_2 as a final step) procedures were used to prepare the surface of the cross sections of the laser tracks. The final surface treatment of the samples for EBSD pattern observations in a Philips XL30S FEG SEM was performed in a Precision Ion Polishing System (PIPS^{TM}) Model 691. Ar^+ ions polished the surface of a rotating sample by bombarding at very low angle (0.5–1°) at voltage of 4 kV.

Interactive as well as automatic indexing of the Electron Back-Scattering Patterns (EBSPs) were used to collect data during a line and rectangular area scans utilizing the software of TexSEM Laboratories, Inc.

Optical microscope (Olympus Vanox-AHTM) and confocal microscope (μSurf, Nanofocus Messtechnik GmbH, Duisburg) with Olympus 50×/0.80 lens was used to observe the progress in ion polishing. A JEOL-4000EX/II high-resolution transmission electron microscope was used to compare the results with the EBSD observations.

3. EBSD sample preparation and results

Fig. 1a shows an optical micrograph of a mechanically polished surface of SiC/Al MMC. The SiC particles are surrounded with a small (∼1 μm) Al_4C_3 reaction zone. Some large (∼30 μm) and thin (∼0.3 μm) plates of Al_4C_3, randomly distributed in the resolidified Al melt pool matrix, are also visible.

Electron Back Scattering Patterns (EBSP) are generated by the interaction of the primary electron beam with a tilted specimen (70 degrees in our observations)

*Author to whom all correspondence should be addressed.

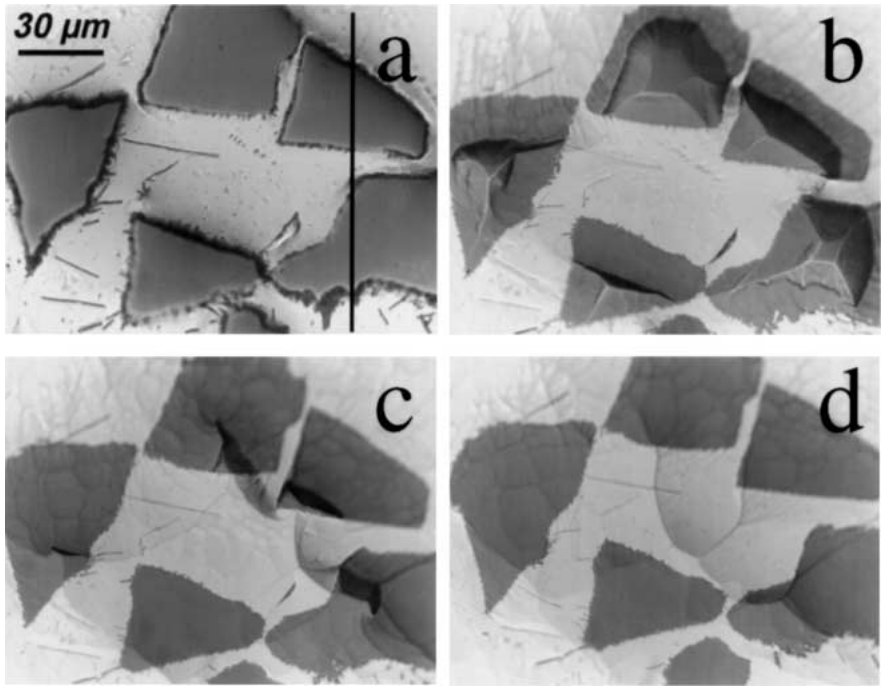

Figure 1 Optical micrographs of SiC/Al MMC prepared by laser melt injection process. The same place of the cross section after (a) mechanical polishing and at different stages of Ar^+ ion polishing: (b) 20 min, (c) 40 min and (d) 60 min. A new system of craters and hillocks independent on the chemical composition of the surface can be easily observed on (d). Vertical line on (a) marks a direction along which a high profile was studied by confocal microscope.

and the typical beam/specimen interaction depth is about 10 nm [7]. These two facts cause that the sample preparation procedure for MMC materials is complicated. The small interaction depth of the electron beam requires a fine polishing or electropolishing of the metallographically prepared surfaces. However, a big difference between mechanical and chemical properties of the ceramic and metal component of the MMC generates steps on the mechanically polished surface at the particle/matrix interface. These steps may hamper clear EBSP observations on the tilted sample. In particular, because of these steps, crystallographic information from the reaction zone at the particle/matrix interface is not straightforward.

Another difficulty is that the EBSP quality, due to the surface quality (roughness and defects), of both SiC and Al phases was not enough to index the patterns properly.

Ion beam milling is another sample preparation method recommended for EBSD [7, 8]. A low bombarding angle (0.5–1°) was chosen to avoid the formation of a step between the ceramic particle and the metal matrix. The effect of the ion polishing process is shown in Fig. 1b–d. The mechanically polished surface from Fig. 1a represents the initial state and Fig. 1b–d shows the surface during the increasing polishing time. Simultaneously the height profile was observed by using a confocal microscope. Fig. 2 shows the evolution of this profile along "a constant" vertical line located in Fig. 1a. At the first stage of ion polishing the steep edges (∼4 μm) of SiC particles move to the center of particles and the size of steps gradually decreases. After 60 minutes of ion polishing the roughness of surface is completely changed and forms a new system of craters and hillocks [9], with lower height differences (∼1 μm) and their position does not depend more on the chemical composition of the surface (see Fig. 1d). Thus

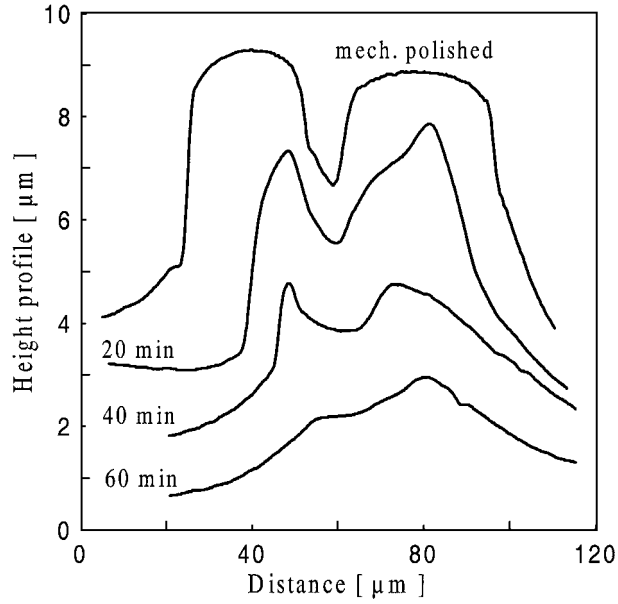

Figure 2 Relative height profiles along the vertical line shown in Fig. 1 (a) measured by confocal microscope after mechanical polishing as well as after different stages of ion beam polishing.

the surface roughness in the area of SiC/Al interface is substantially smaller than in the case of mechanical polishing. Moreover, the surface quality is sufficient to perform the EBSD analysis.

Fig. 3 shows the tilted SEM micrograph of the surface after ion polishing together with an Orientation Imaging Micrograph (OIM) taken from a selected area. The insert in Fig. 3 represents the so-called Image Quality (IQ) map in which darker gray shades denote lower IQ values. Elements with higher atomic numbers generally produce stronger patterns due to increased scattering and this is the main reason for high contrast between

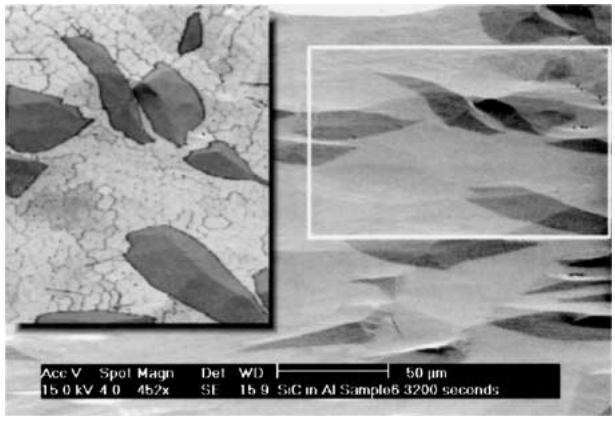

Figure 3 SEM of the ion polished surface of SiC/Al MMC tilted to 70 degrees. Left side insert is OIM picture from marked area with the scan step of 1.1 μm. SiC particles as well as individual Al dendrites and grains are visible. Straight lines, randomly distributed in the matrix belong to Al_4C_3 carbide plates.

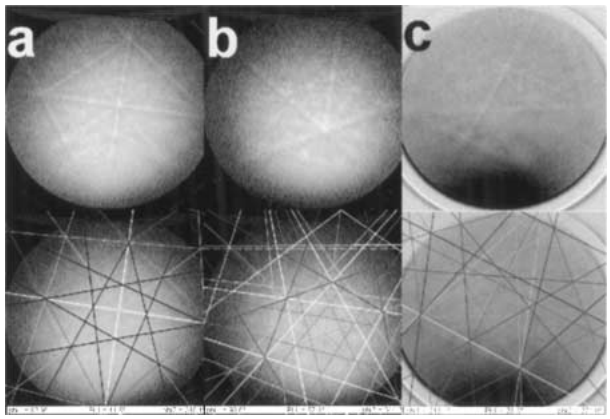

Figure 4 EBSP from phases detected in SiC/Al MMC and their corresponding index lines: (a) Al, (b) SiC, (c) Al_4C_3.

Al matrix and SiC particles. IQ also depends on the local roughness due the deviation in the surface plane from the ideal 70 degrees tilt for diffraction. This is the reason why individual facets of the same SiC particle give different qualities of patterns even though each SiC particle is a single crystal. A low quality signal is obtained from the boundaries between individual Al dendrites as well as from grain boundaries, because EBSP in these places is formed from two or more different oriented crystals. Finally Al_4C_3 plates lying randomly in the Al matrix are also visible on this OIM scan as darker lines with lower quality image. Different crystallographic structure as well as small thickness of these plates is responsible for low quality image.

Fig. 4 shows the typical EBSP for all three phases with corresponding indexing in inserts. Phase differentiation was achieved by automatic indexing a pattern according to the crystal structure parameters for each possible phase, i.e. SiC, Al and Al_4C_3. The indexing results were classified according to a ranking factor based on the number of votes [10] and the fit parameter. The votes give the most probable solution out of all possible solutions; the fit parameter is defined by the average angular deviation between all possible triplets of recalculated and detected bands. Since the phases have different crystal structures this procedure is sufficient to identify the phase and to obtain the correct orientation.

TABLE I Electron diffracting planes for SiC and Al_4C_3 used to index the EBSPs

SiC tuned from X-Ray database Hexagonal, $P6_3mc(186)$, $a = 3.08$ Å, $c = 15.09$ Å					Al_4C_3 calculated Trigonal, R $\bar{3}$ m (166), $a = 3.33$ Å, $c = 24.99$ Å				
h	*k*	*i*	*l*	Intensity	*h*	*k*	*i*	*l*	Intensity
1	0	$\bar{1}$	2	100	1	1	$\bar{2}$	0	100
1	0	$\bar{1}$	1	40	0	0	0	12	94
1	1	$\bar{2}$	6	40	0	1	$\bar{1}$	2	74
1	1	$\bar{2}$	0	35	1	0	$\bar{1}$	7	70
1	0	$\bar{1}$	3	20	0	1	$\bar{1}$	14	62
1	0	$\bar{1}$	9	15	0	3	$\bar{3}$	0	54
0	0	0	12	7	1	0	$\bar{1}$	1	54
					1	0	$\bar{1}$	10	51
					1	1	$\bar{2}$	12	50
					0	1	$\bar{1}$	5	40

In the case of SiC phase the set of diffracting planes based on intensities measured by X-rays diffraction was used as a first approximation. Then manual tuning was applied to identify the right set of diffracting planes for electron diffraction. A trial and error method was performed to add a new diffraction plane to recognize a band, which is not indexed, or to remove redundant one in EBSPs received for different SiC grain orientations.

For the Al_4C_3 phase we calculated the diffraction intensities for electron diffraction, by introducing the atomic positions of the Al_4C_3 unit cell [11] and using the kinematical theory [12]. Table I shows all used set of diffracting planes for both phases. Since Al has a cubic structure the patterns could be indexed using four diffracting planes. These planes were obtained from the software database.

A typical three-phase area scan of a particle matrix interface region is shown in Fig. 5. The left part of Fig. 5 shows the SEM micrograph of the scanned reaction zone, the right part shows the corresponding phase map. The SiC particle, Al matrix and Al_4C_3 reaction layer can be distinguished. The step size is 0.13 μm, the system stores the orientation with respect to the sample axes, phase and image quality for every point inside the scan. The corresponding 0001 pole figures of SiC and Al_4C_3 are depicted in respectively Fig. 6a and b. These pole figures indicate that there is a tendency that the Al_4C_3 basal planes are parallel to the SiC basal planes.

Besides the time consuming area scans, line scans are also performed to analyze more Al_4C_3 grains in order to get better statistics. In this way over a hundred of SiC/Al_4C_3 interfaces, from different SiC particles, are scanned. 25% of the cases fulfil the relation $\{0001\}_{SiC} // \{0001\}_{Al_4C_3}$. Whether this relation arises depend on the SiC orientation since the Al_4C_3 plates prefer to grow with their basal planes parallel to the temperature gradient, which is perpendicular to the SiC/Al_4C_3 interface. Therefore, the more the basal planes of the SiC particle are perpendicular to the SiC/Al_4C_3 interface the less mentioned relation is found.

Parallel SiC and Al_4C_3 basal planes we also observed in transmission electron microscopy (TEM), as shown in Fig. 7. The advantage of OIM in SEM, compared to

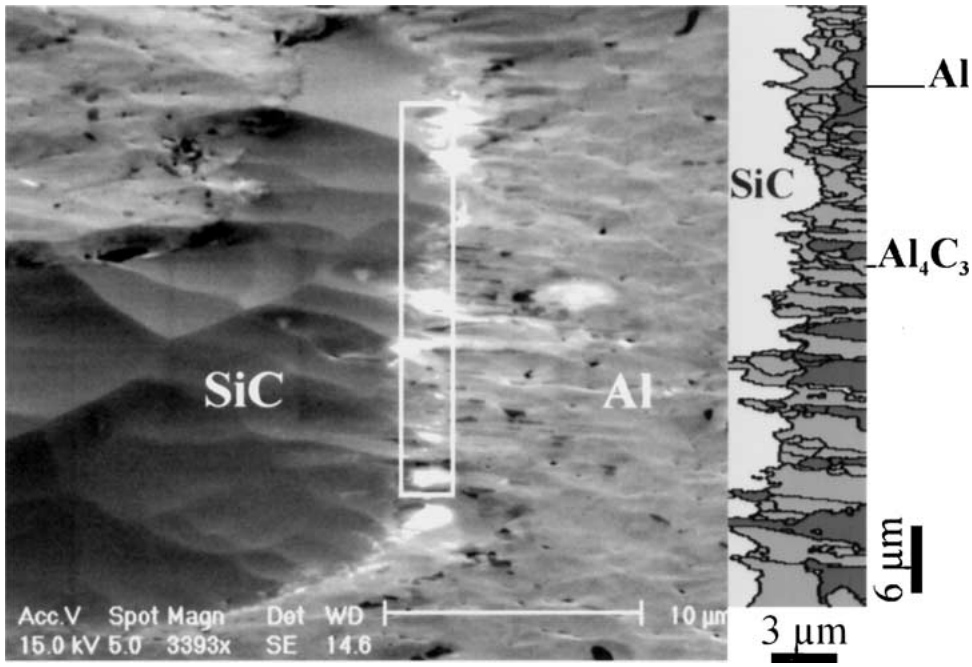

Figure 5 SEM micrograph captured under a tilt angle of 70°. On the right side is the phase map of OIM scan, performed on particle/matrix interface region depicted on SEM picture.

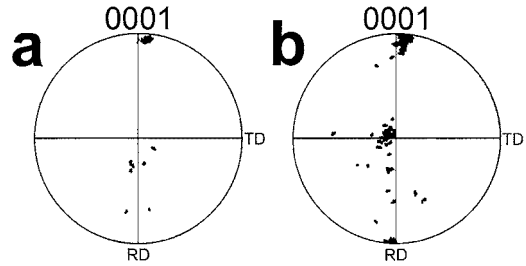

Figure 6 Pole figures of a) SiC and b) Al_4C_3 received from the analysis of EBSD observation on Fig. 5. RD (Roling Direction) and TD (Transverse Direction) are the sample axes.

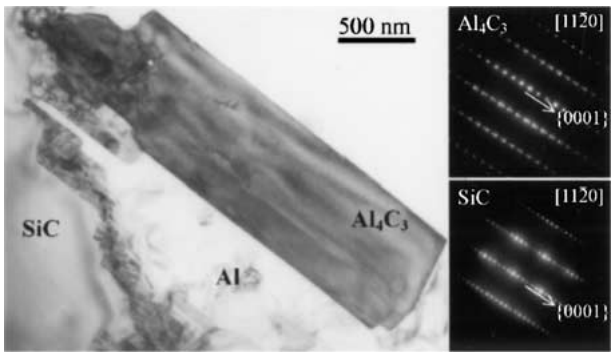

Figure 7 TEM micrograph of an Al_4C_3 plate in the reaction layer with corresponding diffraction patterns, showing the parallel basal planes.

electron diffraction in TEM, is that a larger area can be analyzed and therefore a complete impression of the sample can be obtained, although the accuracy of relative orientation angle between crystals measured by OIM is a little bit low accurate, on the level of 0.5° [7].

4. Discussion

The ion polishing method shows to be appropriate for multiphase materials containing phases with different properties. Standard polishing usually forms steps on the polished surface of such materials. These steps are serious obstacles for EBSP observation, particularly when the contact area of the different materials should be observed. Although the shallow dimples formed on the ion polished surface deflect locally the surface from an ideal back-scatter angle, they are not a big objection for EBSD. This may cause that some of scanned points are not indexed correctly, as some isolated dots in the lower part of SiC particle pole diagram in Fig. 6a demonstrate.

The microstructural observations show that SiC reinforcement particles and their surfaces do not nucleate Al dendrites and do not affect the Al grain size in the laser track. The particles are trapped in the interdendritic regions during final solidification. Therefore no orientation relationship was detected between the particles and Al matrix grains. Large Al_4C_3 plates lying in the matrix are oriented randomly and are incoherent with the matrix, as in-situ fracture observations have revealed [4]. This is completely different to the SiC/Al MMC prepared by cold pressing of SiC powder and subsequent hot extrusion [13, 14]. In this MMC no reaction layer, between particles and matrix was reported and orientation relationships between SiC particles and Al matrix were found. The temperature of hot extrusion is kept well below the melting point of pure Al, but as Viala at al. showed at temperatures above 923 K aluminum carbide phase is formed in a very wide temperature interval [15]. We suppose that large Al_4C_3 plates are formed from free carbon, which is always present in commercial SiC or which originates from thermal decomposition of SiC. On the other hand, small Al_4C_3 plates are the result of a reaction between the solid SiC interface and liquid Al. The second product of the reaction, Si, is present as an Al-Si eutectic in the inter-dendrite area.

Interfacial characteristics between the ceramic particles and metal matrix play a significant role in

determining the mechanical properties. Formation of Al_4C_3 at the carbide/matrix interface is a result of the interfacial reaction between the Al matrix and SiC. Al_4C_3 is known to be very brittle and unstable, resulting in the degradation of the mechanical properties of the composites. Due to the hydrophilic nature of Al_4C_3, composites containing it are very sensitive to some corrosive environments [5, 16]. As Lee *et al*. summarized [16], Si addition into the Al matrix, coating the SiC particles or passive oxidation are methods proposed to avoid Al_4C_3 phase formation. Unfortunately, these methods do not work in the laser melt injection process. The solidification process inside the laser track is realized very far from equilibrium; therefore an addition of Si into Al matrix does not change the solidification process substantially. Similar amounts of aluminum carbides are observed in MMCs prepared by LMI of SiC particles into Al substrate with 8 at.% Si. Protecting the particles with a coating also does not help, because intensive heating up when particle surface is in contact with laser beam usually damages the coating.

The large amount of coherent small Al_4C_3 plates on the surface of SiC probably causes particle cracking. This was observed as a crack initiation process in SiC/Al MMC prepared by LMI [4]. Two close plates, being opened at their ends by the tensile stress in the matrix, act as a wedge block at their roots on the particle surface. Fractographic features that indicate such mechanism for initiation of SiC cleavage were already observed and discussed [4].

5. Conclusions

Precision ion polishing with very low beam angles is an appropriate technique for preparation of the surface of multiphase materials for EBSD observation. Software for automatic indexing of EBSP can be used after careful tuning also for multiphase materials. The combination of these two techniques seems to be a powerful tool to study the orientation relationship in metal matrix composites and multiphase materials generally.

The statistical character of orientation relationship between Al_4C_3 plates formed on the surface of SiC particles and particle itself was confirmed by EBSD technique.

Acknowledgements

Financial support from the foundation for Fundamental Research on Matter (FOM-Utrecht) and the Netherlands Institute for Metals Research are gratefully acknowledged. Henk Bron and Uko Nieborg are thanked for their assistance in sample preparation and Peter Balke is thanked for his OIM experience.

References

1. K. P. COOPER and J. D. AYERS, *Surface Engineering* **1** (1985) 263.
2. J. A. VREELING, V. OCELÍK, Y. T. PEI, D. T. L VAN AGTERVELD and J. TH. M. D. E. HOSSON, *Acta Mater.* **48** (2000) 4225.
3. A. B. KLOOSTERMAN, B. J. KOOI and J. TH. M. D. E. HOSSON, *ibid.* **46** (1998) 6205.
4. J. A. VREELING, V. OCELÍK, G. A. HAMSTRA, Y. T. PEI and J. TH. M. D. E. HOSSON, *Scripta Mater.* **42** (2000) 589.
5. J. K. PARK and J. P. LUCAS, *ibid.* **37** (1997) 511.
6. J. A. VREELING, V. OCELÍK, Y. T. PEI and J. TH. M. D. E. HOSSON, in "Surface Treatment IV," edited by C. A. Brebbia and J. M. Kenny (Computational Mechanics Publications, Southampton, 1999) p. 269.
7. D. J. DINGLEY and V. RANDLE, *J. Mater. Sci.* **27** (1992) 4545.
8. S. GULBRANDSEN-DAHL, G. HEIBERG, J. HJELEN, K. NOGITA, M. RAANES, A. K. DAHLE and L. ARNBERG, in Proceedings of EUREM 12, Brno, Czech Republic, July 8–14, 2000, p. 577.
9. Á. BARNA., G. RADNÓCZI and B. PÉCZ, in "Handbook of Microscopy, Applications in Materials Science, Solid-State Physics and Chemistry," edited by S. Amelinckx, D. van Dyck, J. van Landuyt and G. van Tendeloo (VCH, Weinheim, 1997) p. 751.
10. S. I. WRIGHT and B. L. ADAMS, *Metall. Trans.* **A 23** (1992) 759.
11. G. A. JEFFRY and V. Y. WU, *Acta Cryst.* **20** (1966) 538.
12. B. D. CULLITY, in "Elements of X-Ray Diffraction" (Addison-Wesley, London, 1967) p. 514.
13. M. VAN DEN BURG and J. TH. M. D. E. HOSSON, *Acta Metall. Mater.* **40** Suppl. (1992) S281.
14. R. J. ARSENAUT and J. C. ROMERO, *Scripta Met. Et Mater.* **32** (1995) 1783.
15. J. C. VIALA, P. FORTIER and J. BOUIX, *J. Mater. Sci.* **25** (1990) 1842.
16. J. C. LEE, J. P. AHN, J. H. SHIM, Z. SHI and H. I. LEE, *Scripta Mater.* **41** (1999) 895.

Received 27 December 2000
and accepted 31 May 2001